Dalton Transactions

Accepted Manuscript

ROYAL SOCIETY OF CHEMISTRY

www.rsc.org/dalton

Cite this: DOI: 10.1039/c0xx00000x

www.rsc.org/xxxxxx

ARTICLE TYPE

Solvents and auxiliary ligands co-regulate three antiferromagnetic Co(II) MOFs based on a semi-rigid carboxylate ligand

Lin Cui, Guo-Ping Yang, Wei-Ping Wu, Hui-Hui Miao, Qi-Zhen Shi and Yao-Yu Wang*

Received (in XXX, XXX) Xth XXXXXXXXX 20XX, Accepted Xth XXXXXXXXX 20XX

DOI: 10.1039/b000000x

By reacting an asymmetry semi-rigid Y-shaped/L-shaped linker H_3cpta (H_3cpta = 3-(4'-carboxyphenoxy)phthalic acid) and $Co(CH_3COO)_2{\cdot}6H_2O$ under different N-donor ligands in different solvents, three new Co-based coordination polymers, $[Co_3(cpta)_2(bpe)_3(H_2O)_4]$ (**1**) $[Co(\mu_2\text{-}H_2O)(\mu_3\text{-}OH)(Hcpta)(bpe)(H_2O){\cdot}3(DMF)3(H_2O)]$ (**2**) and $[Co_3(cpta)_2(bpa)_4]$ (**3**) have been obtained. They exhibit trinodal topological nets/layer, based on Co^{2+} ions and Y-shaped/L-shaped carboxylate linkers. **1** and **3** present 3D frameworks with the point symbol $\{4.10^2\}_2\{10^5.12\}\{4.8^5\}_2$ for **1** and $\{4.8^2\}_2\{8^5.9\}\{4.6^7.9^2\}_2$ for **3**. While, **2** exhibits a 2D layer with the point symbol $\{4.6.8\}\{4.6^2.8^3\}\{6^2.8\}$. The magnetic studies indicate that all of the three complexes show antiferromagnetic exchanges transmitted through μ_3-carboxylate/μ_4-carboxylate bridges, μ_2-H_2O molecules and μ_3-OH ions between Co^{2+} ions, respectively. And the result of this research shows that the solvent and the secondary ligands could co-regulate coordination polymer with interesting properties, providing a constructive guidance when synthesizing versatile topologies with same organic spacer but different architecture.

Introduction

On account of the potential applications in molecule magnetism, ion exchange, catalysis, gas storage, nonlinear optics and luminescence, great numbers of synthetic chemists have focused their interest on the rapidly expanding field of the coordination polymers.[1] An effective strategy to obtain coordination polymers (CPs) with functions mentioned above is self-assembly method, in which the metal salts and the organic spacers such as carboxylates are mixed in one-pot reaction. Nevertheless, there still existing a huge challenge in the self-assembly synthesis of CPs is how to predict the final structures of compounds, because the reaction process might be influenced by numbers of factors, such as temperatures, solvents, metal-ligand ratio, counter ions, the nature of spacers, pH values and even supramolecular interactions.[2] Although polycarboxylate ligands can bridge rigid metal clusters as nodes into CPs with structurally predictable frameworks, the variable coordination geometry of the carboxylate can easily link single metal ions in different modes into frameworks of unpredictable topologies.[3]

Recent researches have shown that the so-called semirigid V-shaped multicarboxylate ligands with two aromatic rings bridged by a nonmetallic atom (C, O, S, or N atom) as central molecular framework are of great flexibility, which could be able to lead to metal complexes with diverse structures because of the free rotation of two benzene rings around the bridged nonmetallic atom. While, the symmetric semi-rigid V-shaped multi-dentate O-donor ligands with two of four carboxylic substituents attached at the symmetric positions of semi-rigid V-shaped central molecular framework usually generate coordination polymers with discrete metal ions as node, leading to the limitation in tuning the structure and functionality of coordination polymers (CPs).[4] Therefore, efforts have been started recently to be devoted to the construction of CPs using asymmetric semi-rigid V-shaped multi-dentate O-donor ligands with carboxylic substituents attached at asymmetric positions of central V-shaped molecular framework, obtaining interesting framework with diverse structures and potential application in the field of separation, magnetism, absorption, catalyst and sensors.[5] In contrast to the extensive studies over the CPs formed from symmetrical V-shaped organic ligands, asymmetrical semi-rigid V-shaped multi-dentate O-donor ligands with different numbers of carboxylic substituents at each benzene ring of the central molecular framework have been relatively less investigated.[6] Despite the isolation of interesting CPs comprised of polymetallic clusters and nanotube subunits on the basis of preliminary study employing mixed V-shaped asymmetric multicarboxylate and N-donor ligands reacting with transitional metal ions, it seems still significant to provide more novel organic–inorganic hybrid complexes with a different assembly principle toward further clarifying the relationship between the symmetry of V-shaped multi-dentate O-donor ligands and the structures of CPs under different solvents. Therefore, an asymmetry semi-rigid Y-shaped/L-shaped linker H_3cpta (H_3cpta = 3-(4'-carboxyphenoxy)phthalic acid) (**Scheme 1**) is used to construct frameworks with more versatile topologies.

In this work, two 3D CPs $[Co_3(cpta)_2(bpe)_3(H_2O)_4]$ (**1**) and $[Co_3(cpta)_2(bpa)_4]$ (**3**), one 2D layer coordination polymer $[Co(\mu_2\text{-}H_2O)(\mu_3\text{-}OH)(Hcpta)(bpe)(H_2O){\cdot}3(DMF)3(H_2O)]$ (**2**) have been synthesized under hydrothermal/solvthermal method

with different N-donor ligands-bpe, bpa (**Scheme 1**), which feature different trinodal topologies respectively. The Co(II)-based MOFs often exhibit excellent magnetic properties[1], so the magnetic properties of the three CPs are investigated as well.

Experimental Section

All chemicals and solvents are commercially available and used as received without further purification. Elemental analyses for C, H, and N were determined with a Perkin-Elmer 2400C Elemental Analyzer at the Analysis and Test Research Center of Northwest University. Thermalgravimetric analyses (TGA) were carried out in nitrogen stream using a Netzsch TG209F3 equipment at a heating rate of 5 K/min. Powder X-ray diffraction (PXRD) data were recorded on a Bruker D8 ADVANCE X-ray powder diffractometer (Cu-Kα, λ = 1.5418 Å). Magnetic properties were tested on a Quantum Design MPMS-XL-7 SQUID magnetometer.

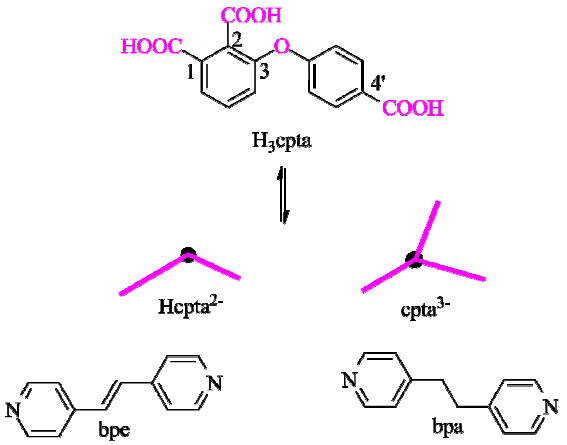

Scheme 1. Schematic Molecular Structures of H_3L and N-donor Ligands

Synthesis of [Co$_3$(cpta)$_2$(bpe)$_3$(H$_2$O)$_4$] (1). A mixture of $Co(CH_3COO)_2{\cdot}6H_2O$ (0.049 g, 0.20 mmol), H_3cpta (0.031 g, 0.10 mmol), bpe (0.037 g, 0.20 mmol) and NaOH (0.10 mL, 0.5 mol·L^{-1}) in H_2O (10 mL) was stirred at room temperature for 30 min after then the mixture was transfered to a Teflon-lined stainless steel vessel (20 mL).The vessel was heated at 418 K for 72 h, then cooled to room temperature at a rate of 5 K/h, giving the pink block crystals of 1, which were isolated by washing with H_2O, and dried in air. The yield $C_{66}H_{52}Co_3N_6O_{18}$ was ca. 67.9 mg (48.7 %, based on the amount of H_3cpta). Anal. Calcd. for : C, 56.87; H, 3.76; N, 6.03. Found: C, 55.30; H, 3.22; N, 6.33 %. IR (KBr, cm^{-1}): 3433 m, 3218 m, 3039 w, 1604 vs, 1549 s, 1401 vs, 1211 w, 1064 m, 831 m, 763 m.

Synthesis of [Co$_2$(μ_2-H$_2$O)(μ_3-OH)(Hcpta)(bpe)(H$_2$O)·3(DMF)3(H$_2$O)] (2). A mixture of $Co(CH_3COO)_2{\cdot}6H_2O$ (0.049 g, 0.20 mmol), H_3cpta (0.031 g, 0.10 mmol), bpe (0.037 g, 0.20 mmol) and NaOH (0.10 mL, 0.5 mol·L^{-1}) in DMF (2 mL) and H_2O (8 mL) was stirred at room temperature for 30 min after then the mixture was transfered to a Teflon-lined stainless steel vessel (20 mL). The vessel was heated at 418 K for 72 h, then cooled to room temperature at a rate of 5 K/h, giving the purple block crystals of 2, which were isolated by washing with DMF, and dried in air. The yield $C_{36}H_{50}O_{16}N_5Co_2$ was ca. 45.4 mg (49.0 %, based on the amount of H_3cpta). Anal. Calcd. for : C, 46.66; H, 5.44; N, 7.56 %. Found: C, 47.31; H, 5.30; N, 7.80. IR (KBr, cm^{-1}): 3440 m, 1598 vs, 1383 vs, 1248 w, 1101 m, 830 m, 763 m, 695 m.

Synthesis of [Co$_3$(cpta)$_2$(bpa)$_4$] (3). A mixture of $Co(CH_3COO)_2{\cdot}6H_2O$ (0.049 g, 0.20 mmol), H_3cpta (0.031 g, 0.10 mmol), bpa (0.037 g, 0.20 mmol) and NaOH (0.10 mL, 0.5 mol·L^{-1}) in H_2O (10 mL) was stirred at room temperature for 30 min after then the mixture was transfered to a Teflon-lined stainless steel vessel (20 mL). The vessel was heated at 418 K for 72 h, then cooled to room temperature at a rate of 5 K/h, giving the pink block crystals of 3, which were isolated by washing with H_2O, and dried in air. The yield of $C_{78}H_{62}Co_3N_8O_{14}$ was ca. 62.3 mg (41.2 %, based on the amount of H_3cpta). Anal. Calcd. for : C, 61.95; H, 4.13; N, 7.41. Found: C, 61.03; H, 4.27; N, 7.38 %. IR (KBr, cm^{-1}): 3416 m, 3053 w, 1610 vs, 1561 s, 1432 vs, 1236 w, 1064 m, 812 m, 757 m.

X-Ray Crystallography. The diffraction data were collected at 296(2) K for **1** and **2**, 293(2) K for **3** with a Bruker AXS Smart Apex diffractometer using ω rotation scans with a scan width of 0.3° and Mo-$K\alpha$ radiation (λ = 0.71073 Å). The structures were solved by direct methods and refined by full-matrix least-squares refinements based on F^2 with the SHELXTL program.[7] All non-hydrogen atoms were refined anisotropically with the hydrogen atoms added to their geometrically ideal positions and refined isotropically. The guest molecules of **2** were highly disordered and could not be located in the structures. Thus the SQUEEZE routine of PLATON was applied to remove the contributions to the scattering from the solvent molecules. The final formulas were determined by combining single-crystal structures, elemental microanalyses and TGA data. Selected crystallographic data and structure refinement results are listed in **Table S1** and **S2**†. A semi-empirical absorption correction was applied using SADABS. The topological analysis and some diagrams were produced using the TOPOS program.[8]

Result and Discussion

Synthesis. The formation of CPs is significantly influenced by the auxiliary ligands, solvent, pH value and so on. As shown in **Scheme 1**, the semi-rigid tricarboxylate ligand was chosen and used to assembly CPs **1** - **3** with the help of the N-donor auxiliary ligands-bpe and bpa (**Scheme 1**). In the present research, **1** and **3** were prepared from the hydrothermal reaction between the tricarboxylate ligand (H_3cpta) and $Co(CH_3COO)_2{\cdot}6H_2O$ together with suitable N-donor ligands, however, Complex **2** was synthesized from the solvothermal reaction between H_3cpta and $Co(CH_3COO)_2{\cdot}6H_2O$ together with bpe. Introducing of the NaOH with a molar ration of 2:1 to the ligand, the reaction between H_3cpta and $Co(CH_3COO)_2{\cdot}6H_2O$ without N-donor auxiliary ligands in different solution gave only some precipitates. However, when the N-donor ligands were introduced, excellent single crystals of three complexes were obtained under suitable solvents, indicating the co-regulation effect of N-donor ligands and the solvents.

Structural Description.

Structure of [Co$_3$(cpta)$_2$(bpe)$_3$(H$_2$O)$_4$] (1). Single-crystals X-ray analysis of **1** reveals that it crystallizes in the triclinic space group *P*$\bar{1}$. The asymmetric unit of **1** contains one and a half crystallographically independent Co^{2+} ions (Co1, 1/2 site occupancy; Co2, entire site occupancy), one fully deprotonation $cpta^{3-}$, three half bpe ligands and two terminal H_2O ligands. Each of Co^{2+} atoms are octahedrally coordination. The difference between the Co1 and Co2 is that Co1 is binded by two pyridyl N atoms from two crystallographically dependent bpe ligands, four carboxylate O atoms two from carboxylates and two H_2O ligands. However, Co2 is coordinated by two pyridyl atoms from two crystallographically indenpendent bpe ligands, three oxygen atoms from two different $cpta^{3-}$ ligands and one oxygen atom from aqua molecule (Figure 1a). The Co–N and Co–O bond lengths are all within the normal ranges. Two Co2 atoms are connected by four $\eta^1:\eta^0:\eta^2:\mu_2$ *syn-syn-syn* carboxylate groups from two $cpta^{3-}$ to afford $Co_2(O_2C)_4(H_2O)_2$ dimmer (Figure 1b) (Co···Co separation of 5.5302 Å). The dimmer has a *C2*-symmetry with the axis traversing the center of the two Co2 atoms. A 4^4 two-dimensional (2D) network is formed by $cpta^{3-}$, Co2 atoms and bpe ligands (Figure 1c) by igorning the connections with Co1 and bpe ligands by which eventually generate the three-dimensional (3D) framework of **1** (Figure 1d).

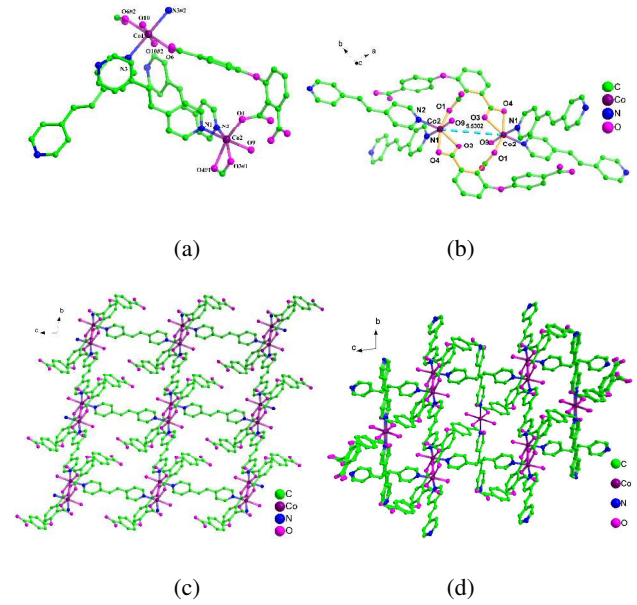

Figure 1 (a) The coordination geometry for Co(II) atoms in 1 with the 30% probability level; all hydrogen atoms and water molecules have been omitted for clarity. (b) The coordination environment of Co2 dimmer in 1. (c) The 2D framework of Co2 by igorning the connections with Co1 and bpe ligands. (d) The three-dimensional framework of 1. [Symmetry codes: #1 = *- x, 1 - y, 1 - z* ; #2 = *1 - x, - y, 2 - z*.]

Structure of [Co(μ$_2$-H$_2$O)(μ$_3$-OH)(Hcpta)(bpe)(H$_2$O)·3(DMF)3(H$_2$O)] (2). A single-crystal X-ray diffraction study of **2** reveals a 2D layer that crystallizes in triclinic space group *P*$\bar{1}$. The asymmetric unit contains only one half of the chemical formula unit, which contains two Co^{2+} ions, one bpe molecule, one μ_2-H_2O molecule, one μ_3-OH anion, one-third of deprotonation $Hcpta^{2-}$ anion, one terminal and two lattice aqua molecules. Two crystallographically independent Co^{2+} ions with same coordination environments binded by one μ_3-OH anion are observed in the structure. As shown in Fig 2a, the Co1 atom is connected by two oxygen atoms from two different carboxylate groups, two oxygen atoms from two μ_3-OH anions, one oxygen atoms from μ_2-H_2O molecule and one nitrogen atom from bpe ligand, giving octahedrally coordination geometry with considerable distrotion. While, the Co2 atom resides in the same distrotion octahedral environment, with the equatorial plane formed by three oxygen atoms from two carboxylate groups and one from μ_3-OH anion bonded with Co1, and the axial position occupied by one pyridyl nitrogen atom from the bpe ligand and one μ_2-H_2O group. Two Co1 and two Co2 are connected with each other *via* two μ_3-OH ions and two μ_2-H_2O molecules, and then formed a $Co_4(\mu_3\text{-}OH)_2(\mu_2\text{-}H_2O)_2(O_2C)_4(H_2O)_2$ core by four μ_2-η^1:η^1-*syn,syn* carboxylate groups and two terminal aqua molecules (Figure 2b top) (Co···Co separation of 3.1864 Å and 3.5813 Å). The Co1-O(H)-Co2 angles are 100.5 and 120.9º, while the angles of Co1-O(H)-Co1 and Co1-O(H_2)-Co2 are 98.8 and 90.0º. Each core is symmetrically joined to adjacent cluster units by two μ_4-carboxylate bridges to form a zigzag metal-oxygen backbone running along the (1,1,1) direction. The adjoining metal-oxygen backbones are further extended to a 2D porous framework through the bpe spacer. The hydrogen bonds between the carboxylate and the lattice water molecules make the 2D adjacent layers connect with each other, generating a three-dimensional (3D) supramolecular network as illustrated in Figure 2d.

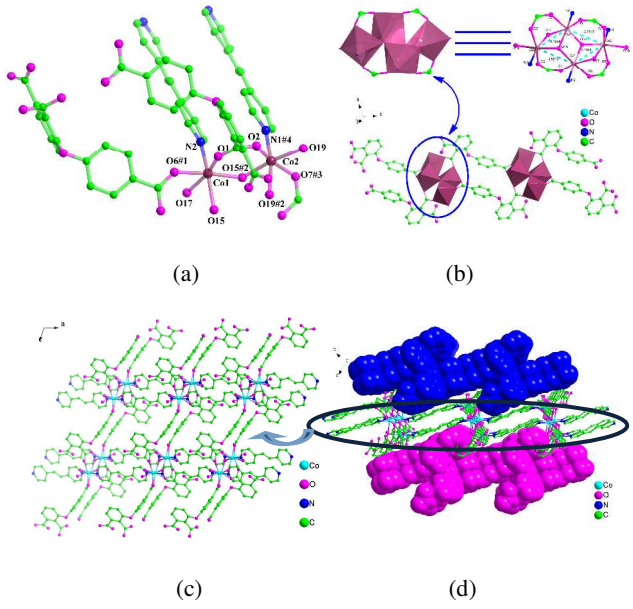

Figure 2 (**a**) The coordination geometry for Co(II) atoms in **2** with the 30% probability level; all hydrogen atoms and water molecules have been omitted for clarity. (**b**) The coordination environment of $Co_4(\mu_3\text{-}OH)_2(\mu_2\text{-}H_2O)_2(O_2C)_4(H_2O)_2$ core in **2**. (**c**) The 2D porous framework of **2**. (**d**) The 3D supramolecular network of **2**. [Symmetry codes: #1 = *- x, - y, - z* ; #2 = *- x, - y, 1 - z* ; #3 = *x, y, 1 + z*; #4 = *1 - x, 1 - y, 1 - z*.]

Structure of [Co$_3$(cpta)$_2$(bpa)$_4$] (3) Crystal **3** crystallizes in the monoclinic system, space group *P2/c*. Single-crystal structure analysis reveals that the asymmetric unit in **3** consists of two independent Co^{2+} cations, one of which is at half occupancy in the asu, the rest being generated by symmetry, one fully-deprotonation $cpta^{3-}$ anion, one and two halves bpa ligand. Of the two Co^{2+} centers, one Co1 is located in a distorted octahedron coordination geometry with the equatorial plane formed by four oxygen atoms from two carboxylate groups, and the axial position occupied by two nitrogen atoms from the bpa ligands. The other Co2 is located in a distorted octahedron geometry with three oxygen atoms from two different $cpta^{3-}$ ligands and one pyridyl atom from bpa ligand at basal positions, and two pyridyl atoms from two different bpa ligands at apical positions as shown in Figure 3a. Co1 atoms are connected with each other by bpa ligands, forming 1D chains, while Co2 atoms forming 2D layers (Figure 3b). Two Co2 centers bridged by two carboxylate in *syn-anti* fashion form a [Co$_2$(O$_2$C-)$_2$] unit, with Co2···Co2 separation of 4.8479 Å (Figure 3c). The Co1 chains and Co2 layers are further linked by μ_3-$cpta^{3-}$ ligands to generate 3D frameworks with Co–O bond distances range from 2.068 to 2.154 Å (Figure 3d).

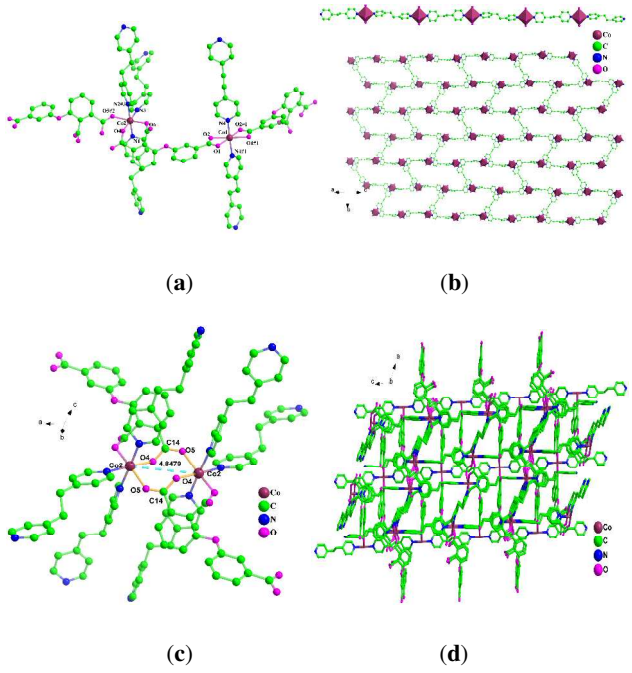

Figure 3 (**a**) The coordination geometry for Co(II) atoms in **3** with the 30% probability level; all hydrogen atoms and water molecules have been omitted for clarity. (**b**) Co1 chain and Co2 layer formed by bpa. (**c**) The coordination environment of [Co$_2$(O$_2$C-)$_2$] unit in **3**. (**d**) The 3D network of **3**. [Symmetry codes: #1 = *2 - x, y, 0.5 - z*; #2 = *- x, 1 - y, - z*; #3 = *x, 1 - y, -0.5 + z*.]

Topological Analysis. Topologically, the $cpta^{3-}$ linkers in **1** and **3** and $Hcpta^{2-}$ linker in **2** all can be simplified as 3-connected nodes, respectively. Remarkably, the 4-connected Co^{2+} nodes in **1** and **3** display significantly distorted octahedral environment, while the Co^{2+} centers show 4- or 5-connected. These nodes combine distorted Y-shaped $cpta^{3-}$ ligands to form a rarely trinodal (3,4,4)-connected net for **1** with the point symbol of $\{4.10^2\}_2\{10^5.12\}\{4.8^5\}_2$ (Figure 4a) and (3,4,5)-connected net for **3** with the point symbol of $\{4.8^2\}_2\{8^5.9\}\{4.6^7.9^2\}_2$ (Figure 4c). However, the Co1 and Co2 atoms in **2** display 3- and 4-connected nodes, these combine the distorted L-shaped $Hcpta^{2-}$ ligands to form a trinodal (3,3,4)-connected layer with the point symbol of $\{4.6.8\}\{4.6^2.8^3\}\{6^2.8\}$ (Figure 4b).

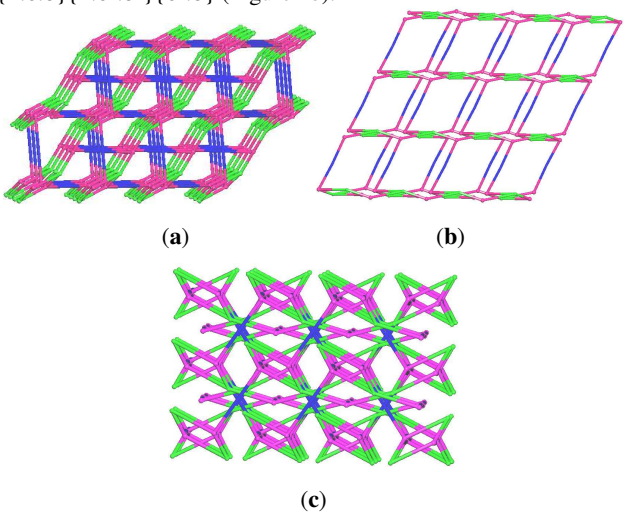

Figure 4 (a) The (3,4,4)-connected net for **1**; (b) The (3,3,4)-connected layer for **2**; (c) The (3,4,5)-connected net for **3**. All of the purple balls represent Co^{2+} ions, while the blue ones for the bpa ligands, and green points represent the cpta ligands.

Coordination Modes. **1** and **2** are synthesized with same initial reactants under different solvents. **1** is hydrothermal synthesized, however **2** is solvothermal with DMF : H_2O (V : V = 1 : 4). Compared to **1** and **2**, **3** is hydrothermal reaction with H_3cpta, $Co(CH_3COO)_2{\cdot}6H_2O$ and bpa. Contrasting the coordination modes among three CPs, carboxylic ligands show μ_3-bridged modes in **1** (Figure 5a) and **3** (Figure 5c), but the connection modes are different. The connection mode in **1** is μ_3-η^2:$\eta^1\eta^0$:$\eta^1\eta^0$-*syn*,*syn*:*syn*:*syn* mode, and that of **3** is μ_3-η^2:$\eta^0\eta^1$:$\eta^1\eta^1$-*syn*,*syn*:*anti*:*anti*,*syn*. However, the mode in **2** displays μ_4-bridged (Figure 5b). The difference between **1** and **2** is the solvents used, and that of **1** and **3** is the N-donor ligands used. The co-regulation of secondary ligands and solvents might accelerates synthesizing CPs with diverse properties.

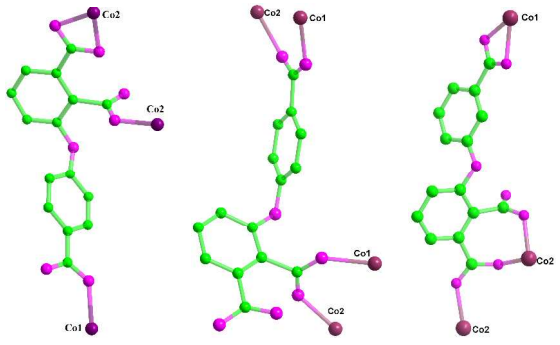

Figure 5 (**a**) μ_3-bridged $cpta^{3-}$ in **1**; (**b**) μ_4-bridged $Hcpta^{2-}$ in **2**;

(**c**) μ_3-bridged cpta^{3-} in **3**. All hydrogen atoms have been omitted for clarity.

The Effect of solvents used and secondary N-donor ligands. Despite the elucidation of the slight difference in the coordination modes in **1** and **3**, the intrinsic reason for the formation for the formation of diverse building units has not been yet been clarified. It therefore appears necessary to further investigate the secondary N-donor ligands on the subunits. The configuration and flexibility of the secondary ligands play a key role in the directing the related properties of the complexes. For **1**, rigid rod-like bpe was selected as an auxiliary ligand, and found to act as a connector to link adjacent 2D Co2-core layers and Co1 chains into a 3D structure. And for **3**, flexible bpa was selected as secondary ligand, which adopt *anti* conformation in the final network (**Scheme 2**), which might cause similar coordination geometry of center ions between **1** and **3**. However, the final structural topology of **3** is quite different with that of **1**, which might due to the flexible secondary ligand used.

Scheme 2. Different Conformations of bpa ligand

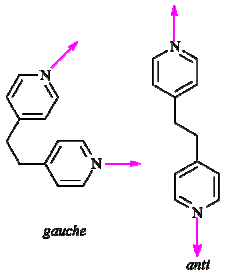

Solvent effect is a vital subject in the construction of coordination polymers. Custormarily, solvents may be broadly classified into two categories of polar and nonpolar, which can be characterized by their dielectric constants. And, it has been well noted that the coordination assemblies of specific reactants will be influenced by solvents used in reactions from both thermodynamic and kinetic aspects, which might yield diverse crystalline products. The structural difference between **1** and **2** may be attributed to the polarity and molecule size of the solvents. H_2O is a polar solvent, which has larger dielectric constant and lower dipole moment, while, DMF has a lower dielectric constant and larger dipole moment, make to be a nonpolar solvent (**Table 1**).[9] The factors mentioned above make water a good proton-donating agent, but DMF a bad proton-donating solvent. And the solvent-encircled H_3cpta molecules are coordinated to metal ions when they collide effectively. H_2O has smaller *van der Waals* volume, which makes molecules collide more effectively, but the larger *van der Waals* volume of DMF make the system collide a little difficult. That's why **1** is 3D structure and **2** is a 2D layer, though the same reactants were mixed initially.

PXRD and Thermal Analysis. To investigate the thermal stability of three compounds, thermal analyses have been carried out on crystalline sample in a nitrogen atmosphere ar heating rate of 10 K min^{-1} (Figure S1 in the Supporting information). TGA of **1** exhibits a significant weight loss of 7.89 % from room temperature to 170 °C (Figure S1†), implying the release all of H_2O solvent molecules per formula unit (calc. 8.29 %), followed an abrupt weight loss followed immediately by the framework collapse. For **2**, the preliminary weight loss of 10.9 % beginning at 240 °C to 290 °C corresponds to the removal of all H_2O ligands (calc. 11.6 %), then followed by a plateau of stability from 290 to 310 °C, and then a weight loss of 14.1 % from 310 to 350 °C corresponds to the removal of all DMF ligands (calc. 13.7 %), whereupon the rapid dissociation of Hcpta^{2-} and bpe induces the framework decomposition. While the TGA of **3** shows a plateau from the beginning to 300 °C, exhibiting a well structural stability, and then followed a rapid dissociation of the framework decomposition. The main framework of **3** is much more stable than those of **1** and **2**, which may attribute to the flexible backbone of bpa ligand that make the network much denser. Match the PXRD patterns of the bulk samples of **1**, **2** and **3** with their simulated patterns from the single-crystal structures, showing the phase purity of the as-synthesized products. The PXRD patterns of all the CPs were performed under Cu-*Kα* radiation (λ = 1.54056 Å). Because there is strong X-Ray fluorescent effect for the compounds contain Mn, Fe, Co, *et. al.* The fluorescent background is difficult to be eliminate. (Figures S2, S3 and S4†).

Table 1 Dlelectric constant, dipole moment,[a] and *van der Waals* volume [b] for DMF and H_2O.

Solvent	Dielectric constant	Dipole moment(D)	*Van der Waals* volume (cm^3 mol^{-1})
DMF	38	3.82	47.67
H_2O	80	1.85	11.44

[a] Data taken from ref. 9*a*. [b] Data calculated using the formula in ref. 9*b*.

Magnetic Property. The variable-temperature magnetic susceptibility (χ_M) of **1**, **2** and **3** were examined in a 1000 *Oe* field in the range 1.8 - 300 K. Because the bridging ligands H_3cpta, bpe and bpa are quite long in **1** and **3**, and thus the Co···Co distances are little long too, the magnetic interaction transferred by these ligands should be very weak. The magnetic properties of **1** and **3** could be regarded as those of a Co2 dimmer and a single metal ion anisotropy. Here, we only give the magnetic property of **1** as an example between **1** and **3**. As shown in Figures 6, 7 and 8, at 300 K, the $\chi_M T$ values of each framework for **1**, **2** and **3** are 10.13, 5.09 and 9.22 cm^3 K mol^{-1}, respectively. The values of **1** and **3** are much higher than the value for three magnetically isolated spin-only S=3/2 Co^{2+} systems (5.625 cm^3 K mol^{-1}), which is as expected because of the significant orbit contribution of high-spin Co^{2+} ion in an octahedral coordination environment. For **1**, upon cooling, the $\chi_M T$ value declines monotonously and reaches 0.12 cm^3 K mol^{-1} at 1.8 K, indicating a significantly antiferromagnetic exchange between the magnetic centers in Co2 dimer. The antiferromagnetic interaction for Co^{2+}-carboxylate dimers is closely related to the Co···Co distances. In the Co2 unit of **1**, the magnetic coupling between Co2 dimmer is transmitted through μ_1-$C_{benzene}$-$\mu_{1,3}$ carboxylate bridges. The long Co···Co distance of 5.5302 Å is resonsible for the antiferromagnetic interaction in **1**, which is also found in other Co2-based complex with carboxylate bridges.[10] The experimental susceptibility data were fitted to the equation that considers the sum of

$Co_2(O_2C)_4(H_2O)_2$ dimmer and mononuclear Co^{2+} ion (eqn. 1), and it is reasonable to explane that (a) the mononuclear Co(N2O4) exhibits a Curie-type magnetic behavior (eqn. 2); (b) the magnetic exchange interaction between dimmers through bridging ligands is quite weak and could be neglected in comparison with magnetic exchange in a dimmer and (c) the magnetic exchange interaction between the dimmer and the neighbour Co(N2O4) can also be ignored. Therefore, the observation that the $\chi_M T$ value decreases upon cooling probably means the existence of an antiferromagnetic exchange interaction in the dimmer or single Co(N2O4) magnetic behavior (Zero-field splitting and spin-orbital coupling , et al.). For the layer binuclear Co^{2+} dimmer, if the spin-orbital coupling interaction is neglected the temperature dependence of the molar magnetic susceptibility could be experssed as eqn (4), where J represents the exchange constant between neighbour Co(N2O4) groups in the $Co_2(O_2C)_4(H_2O)_2$ dimmer and other symbols have their normal meanings.

$$\chi_M = \chi_{dimmer} + \chi_{mononuclear} \quad (1)$$

$$\chi_{mononuclear} = \frac{C}{T} \quad (2)$$

$$C = \frac{Ng^2\beta^2}{4kT} S(S+1) \quad (3)$$

$$\chi_{dimmer} = \frac{2Ng^2\beta^2}{kT} \times \frac{14e^{12J/kT} + 5e^{6J/kT} + e^{2J/kT}}{7e^{12J/kT} + 5e^{6J/kT} + 3e^{2J/kT} + 1} \quad (4)$$

But the molar magnetic susceptibility data of **1** could not be fitted according to the above magnetic exchange model, which is not surprising for the strong spin-orbital coupling interaction of high spin Co^{2+} ion. However, it is difficult to reproduce magnetic susceptibility as a function of temperature when combining magnetic coupling between the neighboring Co^{2+} ions at the same time. In order to estimate the strength of the antiferromagnetic exchange interaction, the following simple phenomenological equation (eqn. 5) can be used, considering the strong spin-orbit coupling in **1**.[11]

$$\chi_M T = A \times \exp(-E_1/kT) + B \times \exp(-E_2/kT) \quad (5)$$

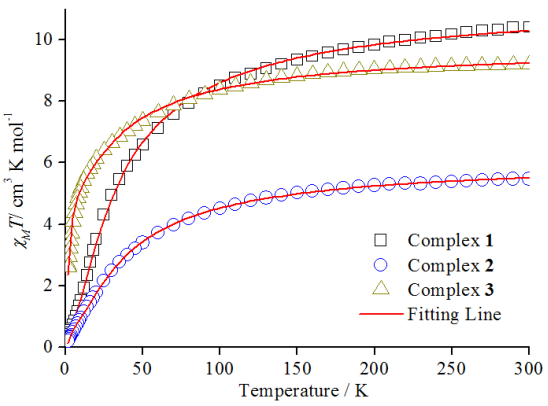

Figure 6. Temperature dependence of $\chi_M T$ for **1** **2** and **3** (opens and red line represent experimental data and fits).

In this equation, $A + B$ equals to the Curie constant, E_1 and E_2 represent the activation energies corresponding to the spin-orbit coupling and the antiferromagnetic exchange interactions, respectively. The equation is in well agreement with the experimental data (Figure 6). The best fitting result is $A + B$ = 11.25 cm^3 K mol^{-1}, E_1/k = 3.7017 K, and $-E_2/k$ = -31.41 K ($R = \sum[(\chi_M T)_{obs} - (\chi_M T)_{calc}]^2/\sum[(\chi_M T)_{obs}]^2$ = 0.008). The obtained value of $A + B$ is very close to that from the Curie-Weiss law equation (11.99 cm^3 K mol^{-1}, Figure S5†) and E_1/k has no significant difference from those given in the literature for the effect of spin-orbit coupling and antiferromagnetic interaction.[10] The value of $-E_2/k$ (-31.41 K) indicates the dominant antiferromagnetic coupling between Co(II) ions as analyzed from the structure of dimmer. For **2**, the best fitting result is $A + B$ = 6.10 cm^3 K mol^{-1}, E_1/k = 4.20 K, and $-E_2/k$ = -37.66 K ($R = \sum[(\chi_M T)_{obs} - (\chi_M T)_{calc}]^2/\sum[(\chi_M T)_{obs}]^2 = 1.11 \times 10^{-2}$) and the obtain value of $A + B$ is very close to that from the Curie-Weiss law equation (6.63 cm^3 K mol^{-1}, Figure S6†). While for **3**, the best fitting result are $A + B$ = 9.15 cm^3 K mol^{-1}, E_1/k = 41.35 K, and $-E_2/k$ = -1.78 K ($R = \sum[(\chi_M T)_{obs} - (\chi_M T)_{calc}]^2/\sum[(\chi_M T)_{obs}]^2 = 8.02 \times 10^{-2}$). As same as **1** and **2**, the obtain value of $A + B$ is very close to that from the Curie-Weiss law equation (9.45 cm^3 K mol^{-1}, Figure S7†).

The $\chi_M T$ values at room temperature between **1** and **3** are almost the same with each other, which is due to the same coordination orientation of bpe and *anti*-bpa. But the $\chi_M T$ values at 1.8 K are much different, which is because of the flexible backbone of the *anti*-bpa, making closer distance of Co ions between Co2 dimmer (**2**, 4.8479 Å; **3**, 5.5302 Å). Comparing the $\chi_M T$ values at room temperature between **1** and **2**, the value of **1** is almost two times than that of **2**, which means a strong spin-orbit coupling. What makes this phenomenon is for the solvent used.

Conclusions

In conclusion, three new magnetic MOFs with semi-rigid carboxylate ligand (3-(4'-carboxyphenoxy)phthalic acid) and different N-donor auxiliary ligands have been synthesized under different solvents conditions. Complex **1** and complex **3** show same μ_3-carboxylate bridges with different linkage type though the same solvent is used, which might be due to the different N-donor ligands. However, **1** and **2** are synthesized with the same reactants and the structural invetsigation shows different

carboxylate bridges because of the solvents used. All of the complexes show antiferromagnetic interaction between Co^{2+} ions. In summary, the research demonstrates a co-regulation effect of auxiliary ligands and the reacting solvents, giving a guiding reference when synthesizing MOFs with attractive properties. And the further investigation of H_3cpta will be studied in our laboratory.

Acknowledgements

This work is supported by State Key Program of National Natural Science of China (No. 20931005), Key Research Planning Program of National Natural Science Foundation of China (Grant No. 91022004), National Natural Science Foundation of China (Grant 21371142 and 21201139), Natural Science Foundation of Shaanxi Province (Grant 2013JQ2016), Science Research Plan Projects of Shaanxi Provincial Educational Department (Grant 12JK0605).

[a] *Key Laboratory of Synthetic and Natural Functional Molecule Chemistry of the Ministry of Education, Shaanxi Key Laboratory of Physico-Inorganic Chemistry, College of Chemistry and Materials Science, Northwest University, Xi'an, Shaanxi, P. R. China. Fax: (+ 86)-29-88303798; E-mail: wyaoyu@nwu.edu.cn*

† Electronic Supplementary Information (ESI) available: [details of any supplementary information available should be included here]. See DOI: 10.1039/b000000x/.

‡ CCDC 965948-965950, for compounds **1**–**3**, contain the supplementary crystallographic data for this paper. These data can be obtained free of charge from The Cambridge Crystallographic Data Centre at www.ccdc.cam.ac.uk/data_request/cif. These data can be obtained freely.

References

1 (a) P. Dechambenoit and J. R. Long, *Chem. Soc. Rev.*, 2011, 40, 3249-3265; (b) H. L. Jiang and Q. Xu, *Chem. Commun.*, 2011,47, 3351-3370; (c) *Metal Organic Frameworks: Applications from Catalysis to Gas Storage*, ed. D. Farrusseng, Wiley, Weinheim, 2011; (d) Z. J. Lin, T. F. Liu, X. L. Zhao and R. Cao, *Cryst. Growth Des.*, 2011, 11, 4284-4287; (e) L. Hou, W. J. Shi, Y. Y. Wang, Y. Guo, C. Jin and Q. Z. Shi, *Chem. Commun.*, 2011, 47, 5464-5466; (f) Z. Z. Lu, R. Zhang, Y. Z. Li, Z. J. Guo and H. G. Zheng, *J. Am. Chem. Soc.*, 2011, 133, 4172-4177; (g) I. Eryazici, O. K. Farha, O. C. Compton, C. Stern, J. T. Hupp and S. T. Nguyen, *Dalton Trans.*, 2011, 40, 9189-9193; (h) M. V. Lucky, S. Sivakumar, M. L. P. Reddy, A. K. Paul and S. Natarajan, *Cryst. Growth Des.*, 2011, 11, 857-864; (i) S. R. Batten, S. M. Neville and D. R. Turner, *Coordination Polymers: Design, Analysis and Application*, Springer, New York, 2010; (j) F. Nouar, J. Eckert, J. F. Eubank, P. Forster and M. Eddaoudi, *J. Am. Chem. Soc.*, 2009, 131, 2864-2870; (k) H. X. Deng, S. Grunder, K. E. Cordova, C. Valente, H. Furukawa, M. Hmadeh, F. Gándara, A. C. Whalley, Z. Liu, S. Asahina, H. Kazumori, M. O'Keeffe, O. Terasaki, J. F. Stoddart and O. M. Yaghi, *Science*, 2012, 336, 1018-1023; (l) D. S. Li, J. Zhao, Y. P. Wu, B. Liu, L. Bai, K. Zou, M. Du, *Inorganic Chemistry*, 2013, 8091–8098; (m) D. S. Li, F. Fu, J. Zhao, Y. P. Wu, M. Du, K. Zou, W. W. Dong, Y. Y. Wang, *Dalton Transactio*n, 2010, 39, 11522-11525.

2 (a) X. M. Zhang, *Coord. Chem. Rev.*, 2005, 249, 1201-1219; (b) B. Moulton, M. J. Zaworoto, *Chem. Rev.*, 2001, 101, 1629-1658.

3 (a) H. Li, M. Eddaoudi, M. O'Keeffe, O. M. Yaghi, *Nature*, 1999, 402, 276-279; (b) G. Ferey, C. Serre, F. Millange, J. Dutour, S. Surble, I. Margiolaki, *Science*, 2005, 309, 2040-2042; (c) D. S. Li, Y. P. Wu, J. Zhao, J. Zhang, J. Y. Lu, *Coordination Chemistry Reviews*, 2014, 261, 1–27

4 (a) M. Eddaoudi, J. Kim, N. Rosi, D. Vodak, J. Wachter, M. O'Keefe and O. M. Yaghi, *Science*, 2002, 295, 469-472; (b) C. Serre, F. Millange, J. Marrot and G. Férey, *Chem. Mater.*, 2002, 14, 2409-2415; (c) H. Chun, H. Jung, G. Koo, H. Jeong and D. K. Kim, *Inorg. Chem.*, 2008, 47, 5355-5359; (d) L. Xu, E. Y. Choi and Y. U. Kwon, *Inorg. Chem.*, 2007, 46, 10670-10680; (e) J. W. Ye, J. Wang, J. Y. Zhang, P. Zhang and Y. Wang, *CrystEngComm*, 2007, 9, 515-523; (f) D. Bradshaw, T. J. Prior, E. Cussen, J. B. Claridge and M. J. Rosseinsky, *J. Am. Chem. Soc.*, 2004, 126, 6106-6114; (g) Z. Lin, D. S. Wragg, J. E. Warren and R. E. Morris, *J. Am. Chem. Soc.*, 2007, 129, 10334-10335. (h) D. R. Xiao, E. B. Wang, H. Y. An, Y. G. Li, Z. M. Su and C. Y. Sun, *Chem.–Eur. J.*, 2006, 12, 6528-6541.

5 (a) X. L. Wang, C. Qin, E. B. Wang, Y. G. Li, Z. M. Su, L. Xu and L. Carlucci, *Angew. Chem., Int. Ed.*, 2005, 44, 5824-5827; (b) P. Mahata, G. Madras and S. Natarajan, *J. Phys. Chem. B*, 2006, 110, 13759-13768; (c) S. L. Li, Y. Q. Lan, J. F. Ma, J. Yang, G. H. Wei, L. P. Zhang and Z. M. Su, *Cryst. Growth Des.*, 2008, 8, 1610-1616; (d) Y. Q. Lan, S. L. Li, K. Z. Shao, X. L. Wang, D. Y. Du, Z. M. Su and D. J. Wang, *Cryst. Growth Des.*, 2009, 9, 1353-1360; (e) X. L. Chen, B. Zhang, H. M. Hu, F. Fu, X. L. Wu, T. Qin, M. L. Yang, G. L. Xue and J. W. Wang, *Cryst. Growth Des.*, 2008, 8, 3706-3870; (f) Q. Chu, G. X. Liu, Y. Q. Huang, X. F. Wang and W. Y. Sun, *Dalton Trans.*, 2007, 4302-4311.

6 (a) Wang, H.; Zhang, D.; Sun, D.; Chen, Y.; Zhang, L. F.; Tian, L.; Jiang, J.; Ni, Z. H. *Cryst. Growth Des.*, 2009, 9, 5273-5282. (b) Wang, H.; Zhang, D.; Sun, D.; Chen, Y.; Wang, K.; Ni, Z. H.; Tian, L.; Jiang, J. *CrystEngComm*, 2010, 12, 1096-1102. (c) Zhang, S. Q.; Jiang, F. L.; Wu, M. Y.; Ma, J.; Bu, Y.; Hong, M. C. *Cryst. Growth Des.*, 2012, 12, 1452-1463.

7 Sheldrick, G. M. SHELXL, version 6.12; Bruker Analytical Instrumentation: Madison, WI, 2000.

8 Blatov, V. A.; Shevchenko, A. P.; Serezhkin, V. N. *J. Appl. Crystallogr.* 2000, 33, 1193.

9 (a) Niu C. Y.; Zheng X. F.; Wan X. S.; Kou C. H. *Cryst. Growth Des.*, 2011, 11, 2874-2888. (b) Ma, L.-F.; Wang, L.-Y.; Du, M.; Batten, S. R. *Inorg. Chem.*, 2010, 49, 365-367.

10 (a) Rueff, J. M.; Masciocchi, N.; Rabu, P.; Sironi, A.; Skoulios, A. *Eur. J. Inorg. Chem.*, 2001, 2843-2848. (b) Wang, X. Y.; Sevov, S. C. *Inorg. Chem.*, 2008,47, 1037-1043. (c) Liang, L. L.; Ren, S. B.; Wang, J.; Zhang, J.; Li, Y. Z.; Du, H. B.; You, X. Z. *CrystEngComm.*, 2010, 12, 2669-2671.

Solvents and auxiliary ligands co-regulate three antiferromagnetic Co(II) MOFs based on a semi-rigid carboxylate ligand

Lin Cui, Guo-Ping Yang, Wei-Ping Wu, Hui-Hui Miao, Qi-Zhen Shi and Yao-Yu Wang*

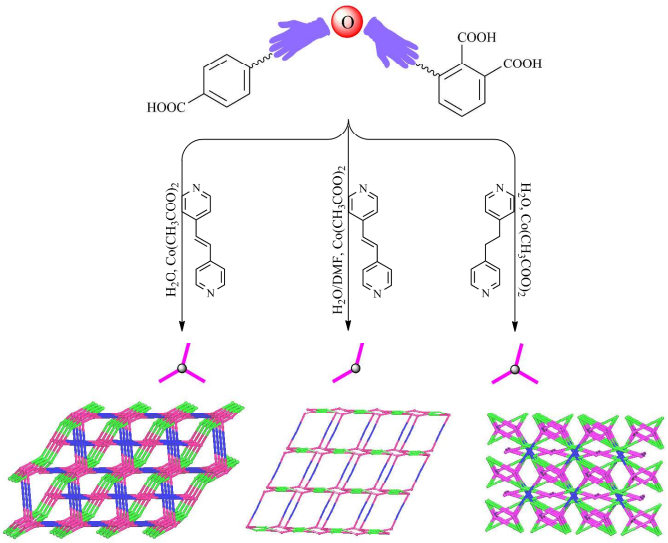

By reacting an asymmetry semi-rigid Y-shaped/L-shaped linker H_3cpta (H_3cpta = 3-(4'-carboxyphenoxy)phthalic acid) and $Co(CH_3COO)_2{\cdot}6H_2O$ under different N-donor ligands in different solvents, three new Co-based coordination polymers, $[Co_3(cpta)_2(bpe)_3(H_2O)_4]$ (**1**) $[Co(\mu_2\text{-}H_2O)(\mu_3\text{-}OH)(Hcpta)(bpe)(H_2O){\cdot}3(DMF)3(H_2O)]$ (**2**) and $[Co_3(cpta)_2(bpa)_4]$ (**3**) have been obtained. They exhibit trinodal topological nets/layer, based on Co^{2+} ions and Y-shaped/L-shaped carboxylate linkers. **1** and **3** present 3D frameworks with the point symbol $\{4.10^2\}_2\{10^5.12\}\{4.8^5\}_2$ for **1** and $\{4.8^2\}_2\{8^5.9\}\{4.6^7.9^2\}_2$ for **3**. While, **2** exhibits a 2D layer with the point symbol $\{4.6.8\}\{4.6^2.8^3\}\{6^2.8\}$. The magnetic studies indicate that all of the three complexes show antiferromagnetic exchanges transmitted through μ_3-carboxylate/μ_4-carboxylate bridges, μ_2-H_2O molecules and μ_3-OH ions between Co^{2+} ions, respectively. And the result of this research shows that the solvent and the secondary ligands could co-regulate coordination polymer with interesting properties, providing a constructive guidance when synthesizing versatile topologies with same organic spacer but different architecture.